Acta Crystallographica Section B
Structural Science, Crystal Engineering and Materials
ISSN 2052-5192

Effect of lone-pair stereoactivity on polyhedral volume and structural flexibility: application to $Te^{IV}O_6$ octahedra

Andrew G. Christy[a]* and Stuart J. Mills[b]

[a]Centre for Advanced Microscopy, Australian National University, Canberra, ACT 0200, Australia, and [b]Department of Geosciences, Museum Victoria, GPO Box 666, Melbourne, Victoria 3001, Australia

Correspondence e-mail: andrew.christy@anu.edu.au

Received 2 April 2013
Accepted 16 August 2013

The Distortion Theorem implies that the irregularity of bond distances in a distorted coordination polyhedron causes an increase of mean bond distance. Examination of 40 polyhedra containing the lone-pair cation Te^{IV} shows that this does not imply an increase in polyhedral volume. Volumes of these polyhedra are 10.3–23.7 Å^3, compared with the 12.83 Å^3 expected for a hypothetical regular octahedron. There is little correlation between volume and measures of polyhedral distortion such as quadratic elongation, bond-angle variance or vector bond valence. However, the oxygens of our polyhedra lie very close to a sphere of best fit, centred at $\sim$1 Å from the Te^{IV} atom. The Te^{IV}–centre distance is an index of lone-pair stereoactivity and is linearly related to the radius R_{sph} of the sphere; this is explained by a more localized lone pair repelling the anions more strongly, leading to a longer non-bonded distance between the lone pair and anions. Polyhedral volume still varies considerably for a given R_{sph}, because the oxygen ligands may be distributed over the whole sphere surface, or confined to a small portion of it. The uniformity of this distribution can be estimated from the distance between the sphere centre and the centroid of the O_6 polyhedron. Te^{IV}–centre and centroid–centre distances alone then account for 95% of the variation observed in volume for polyhedra which are topologically octahedral. Six of the polyhedra studied that are outliers are closer in shape to pentagonal pyramids than octahedra. These have short distances from the central Te^{IV} cation to other Te^{IV} and/or to large, polarizable cations, suggesting additional weak bonding interactions between these species and the central lone pair. The flexibility of lone-pair polyhedra is further enhanced by the ability of a single polyhedron to accommodate different cations with different degrees of lone-pair activity, which facilitates more diverse solid solution behaviour than would otherwise be the case.

1. Introduction

The presence of non-bonding lone pairs of electrons on a central atom has long been known to have a severe perturbing effect on the arrangement of ligands around that atom (*e.g.* Sidgwick & Powell, 1940; Gillespie & Nyholm, 1957). In the valence-shell electron-pair repulsion (VSEPR) model of the latter authors, the lone pair not only plays the stereochemical role of an additional ligand, but also repels bond pairs more than they do each other. Thus, the lone pair subtends a more solid angle at the central atom and is effectively 'larger' than conventional ligands.

Lone-pair repulsion leads to a characteristically asymmetric coordination for the central atom, in which the strongly bound

ligands are all displaced to one side, away from the lone pair. However, the lone-pair atom frequently acquires additional more distant ligands, on the same side as the lone pair. In molecular solids, these may be atoms from more topologically distant parts of the same molecule or atoms in different molecules. In either case, the additional interactions can be significant in stabilizing molecular complexes and packing them to form a three-dimensional structure. In a paradigm where bonds are assumed to be two-centre electron-pair bonds of integral order ≥ 1, interactions with such species are treated as special cases: they have been referred to as 'secondary bonds'. Alcock and co-workers described many instances in an extensive series of papers (*cf.* Alcock & Harrison, 1982; Alcock *et al.*, 1992).

In solids with extended, non-molecular structures, coordination numbers generally are higher than in molecular materials, and bonding departs from the two-centre, integral-order model even in simple structures such as that of rocksalt. It is common for lone-pair cations in extended structures to have numerous weakly bonded neighbours in addition to their primary ligands. The strong 'primary' and weak 'secondary' bonds to neighbours of a central atom with a lone pair become part of a continuum of bonded interactions that show a wide range of bond strengths. Systematic correlations for given pairs of species have been established between bond distance and 'bond valence' (essentially analogous to nonintegral bond order), which may take power-law (*e.g.* Brown & Wu, 1976) or logarithmic form (*e.g.* Brown & Altermatt, 1985; Brese & O'Keeffe, 1991). In the latter case, the bond distance r for a given bond valence s between a given pair of species is given by

$$r = r_0 - b \ln s. \quad (1)$$

The softness parameter b has usually been assigned the value of 0.37 Å irrespective of the species pair (Brown & Altermatt, 1985; Brese & O'Keeffe, 1991), although Brown (2002) notes that larger values may be appropriate for more polarisable species. Further alternative parameterizations are discussed in the review of Brown (2009). A recent introduction to the use of bond-valence theory in modelling coordination geometry has been given by Brown (2013*a*).

Accurate bond-valence parameters are desirable, given their utility in assessing the overall quality of structure determinations and distinguishing isoelectronic species such as O^{2-}, OH^- and H_2O. Therefore, we recently determined revised r_0 and b parameters for Sb^{III}—O and Sb^{V}—O (Mills, Christy, Chen & Raudsepp, 2009) and for Te^{IV}—O and Te^{VI}—O (Mills & Christy, 2013). It is apparent from these data that for the cations with stereoactive lone pairs, there is no qualitative difference between the short–strong 'primary bonds', usually 3–4 in number and oriented away from the lone pair, and the longer 'secondary' bonds. A single set of parameters gives well behaved bond-distance and bond-valence behaviour for all interactions out to our cut-off distance of 3.5 Å. Hence, in the majority of structures containing lone-pair cations, it is possible to define a coordination polyhedron of up to 12 ligands which completely surrounds the cation and the lone pair (*cf.* Mills & Christy, 2013, supplement 1). A good general example of such a polyhedron with bimodal distribution of bond distances and asymmetric positioning of the central cation is given by Te1 in the structure of balyakinite, $CuTeO_3$ (Lindqvist, 1972). This Te cation has a total of 9 oxygen neighbours within 3.5 Å. Three O atoms on the side of Te facing away from the lone pair are at distances < 2 Å and have bond valence > 1, while the six O atoms on the same side as the lone pair are much further away, with very low bond valences (Fig. 1). The lone pair behaves like a small additional anion bonded at a short distance to Te, and repelling other anionic species.

Although lone pairs cannot be distinguished in conventional electron-density maps, they can be visualized when electron-spin correlations are taken into account, using an electron-localization function (ELF) applied to an *ab initio* model of a structure (Becke & Edgecombe, 1990; Seshadri, 2001; Raulot *et al.*, 2002). In ELF contour plots, lone pairs manifest as domains of non-bonding electron density which form caps sitting adjacent to the cores of the lone-pair atom. If the lone pair is highly stereoactive, the cap is small and of high electron density. Conversely, a lone pair with little stereoactivity is spread out until it ultimately becomes a spherical sheath surrounding the core. This picture of the lone pair is more consistent than the pseudo-anion model with the vector bond-valence approach to coordination geometry of Harvey *et al.* (2006) and Zachara (2007), which is discussed briefly below. However, the two models are compatible: the pseudo-anion model for the lone pair corresponds at least qualitatively to the centroid of the lone-pair density as shown by ELF mapping. Fig. 2 compares the two styles of depiction for lone pairs with different degrees of stereoactivity. A highly stereoactive lone pair is shown in Fig. 2(*a*) as a pseudo-anion that is well separated from the nucleus of its parent atom, while a less active lone pair is depicted as a similar sphere lying much closer to the nucleus, embedded in the core electrons of the atom. Conversely, Fig. 2(*b*) shows the active lone pair as a

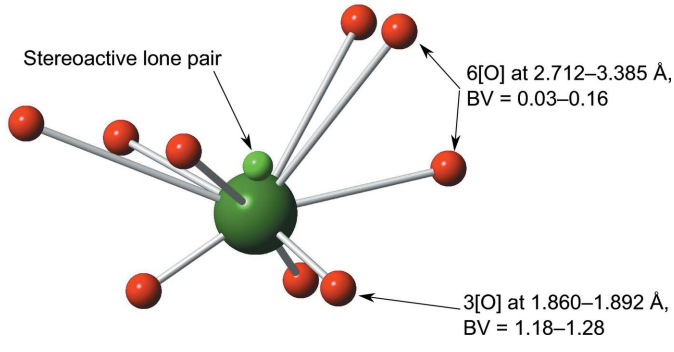

Figure 1
A typical $Te^{IV}O_n$ polyhedron: that of Te1 in balyakinite, $CuTeO_3$. The lone pair is indicated by a small sphere on the side of the central Te atom. Note the separation of the 9 oxygen neighbours into a group of 3 that are at a short distance (< 2.0 Å) with bond valence (BV) > 1, facing away from the lone pair, and a group of 6 on the same side as the lone pair that are much further away (> 2.7 Å) and more weakly bound (BV < 0.2).

small, dense, well localized cap of non-bonding electron density on the atom, while the less-localized lone pair appears as a lower-density cap of non-bonding electrons that spreads over most of the surface of the atom.

Lone-pair activity may be suppressed when other ligands are very numerous and the coordination number high, or when the other ligands are very large (*e.g.* heavy halide and chalcogenide anions), but is frequently seen for sulfides [exceptions include Pb^{II} in galena, PbS and Bi^{III} in kupcikite, $(Cu,Fe)_4Bi_5S_{10}$; Topa *et al.*, 2003]. However, strong lone-pair stereoactivity is almost ubiquitous in oxycompounds; Pb^{II} in rosiaite, $PbSb_2O_6$, is one of the very few exceptions (Basso *et al.*, 1996). Brown (2011) discussed the influence of ligands and their preferred bonding valences on the degree of stereoactivity shown by lone pairs.

In distorted polyhedra the cation is considerably displaced from the centroid of the polyhedron, while the lone pair generally lies closer to the centroid, consistent with its structural role as a quasi-anion which repels the true anionic ligands of the cation. Frequently, the structure can be related to others that do not possess stereoactive lone pairs, either by (i) restoring the cation to the centroid of its coordination polyhedron or (ii) replacing the lone pair at the centroid of the polyhedron with a small anion such as F^- or O^{2-}, and modifying the charge and position of the cation so as to maintain charge balance and create a smaller, symmetrical coordination polyhedron for it. Examples of the first type of relationship are those between the structures of stibnite, Sb_2S_3 (Bayliss & Nowacki, 1972) and α-U_2S_3 (Zachariasen, 1949), or between Pb-dominant and other members of the alunite supergroup of minerals (*cf.* Mills, Kampf, Raudsepp & Christy, 2009; Mills *et al.*, 2009, 2010; Mills & Nestola, 2012). An example of the latter would be between the structures of the massicot polymorph of PbO and the scrutinyite form of PbO_2, as discussed in Hyde & Andersson (1989).

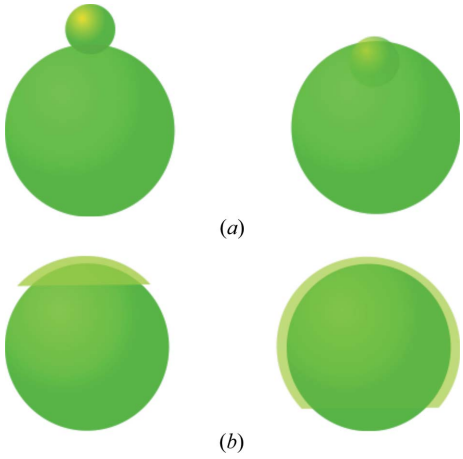

Figure 2
Comparison of two different styles of visualization of lone pairs. Large spheres represent the core electron density of a lone-pair atom in each case. (*a*) A highly stereoactive lone pair shown as a small quasi-anion at a relatively large distance from the nucleus of the atom (left), while a less stereoactive pair is closer to the nucleus, almost subsumed within the core (right). (*b*) The same lone pairs as depicted in ELF contour maps. The stereoactive lone pair appears as a small cap of high nonbonding electron density on one side of the atom core (left), while the less active lone pair is spread into a nearly complete spherical shell surrounding the core (right).

Whatever the functional relationship between r and s, it takes the form of a nonlinear curve that is concave upwards. Therefore, any irregularity in bond distances to a central atom leads to an increase in the mean distance, in order to maintain a constant bond-valence sum on the central atom: this is the well known 'Distortion Theorem' (Allmann, 1975; Brown, 1978; Urusov, 2003). The lengthened mean bond distance would contribute to an increase in volume of the coordination polyhedron, and hence an increase in molar volume of the structure as a whole. However, a polyhedron has several possible modes of distortion available to it, and it may be possible for bond angles to change such that the longer bond distances can be accommodated in a smaller volume rather than a larger one.

In this study, we investigate the relationship between polyhedral volume and the degree of lone-pair stereoactivity for a suite of 40 Te^{IV}—O polyhedra from published structure refinements that are included in the Inorganic Crystal Structure Database (Fachinformationszentrum Karlsruhe, http://icsd.fiz-karlsruhe.de). However, the qualitative conclusions of this study are applicable to any polyhedron distorted by lone-pair stereoactivity, whether the central cation is Te^{IV} or other species such as Pb^{II}, Sb^{III} *etc*.

2. Methodology

The volume effect of lone-pair stereoactivity is readily investigated through a combination of surveying experimental structure determinations with the use of simple theoretical models. In Mills, Christy, Chen & Raudsepp (2009), we considered a model in which a regular coordination polyhedron of O atoms surrounded an Sb^{III} cation, expanded in response to off-centring of the cation. It was shown that cation displacement of approximately 1 Å, regarded as typical for heavy lone-pair species such as Sb^{III} and Te^{IV} by Hyde & Andersson (1989), increased the mean cation–oxygen bond length by nearly 6% and the polyhedral volume by 16%. However, we have since examined the volumes of a range of real coordination polyhedra, and have found that their actual behaviour can be much more varied, as reported in this study.

Mills & Christy (2013) used bond distance data from 208 Te^{IV}—O polyhedra to refine bond-valence parameters r_0 = 1.9605 Å and b = 0.41. The coordination number of Te ranged from 3 to 12, using a Te—O distance cutoff of 3.5 Å, comparable to the shortest cation–cation distances. Since the regular octahedron provides a well defined reference state for zero distortion, we selected for the current study the subset of 40 polyhedra in which Te has exactly six oxygen neighbours (Table 1). A regular $Te^{IV}O_6$ octahedron with a formal valence of 4.0 on Te has the bond distance r = 2.1267 Å and volume = $(4/3)r^3$ = 12.825 $Å^3$.

For this study, polyhedral volume is defined as the volume of the convex hull defined by vertices at the centres of the oxygen ligands and straight-line edges connecting those

Table 1
The $Te^{IV}O_6$ polyhedra investigated in this study, with their volumes.

The asterisks in the left-hand column indicate the polyhedra that have pyramidal rather than octahedral topology.

	ICSD #	Compound	Site	Reference	V_{poly} (Å^3)
1	1	$(Te_4O)Cr_2O_{10}$	Te2	Meunier *et al.* (1976)	14.338
2	293	$Ni_3(OH)_2(TeO_3)_2$	Te1	Perez *et al.* (1976)	16.028
3	294	$Co_3(OH)_2(TeO_3)_2$	Te1	Perez *et al.* (1976)	15.882
4	2397	$(NH_4)_2Te_2O_5(H_2O)_2$	Te2	Johansson (1978)	16.169
5	8283	$Fe_2Te_3O_9$	Te3	Astier *et al.* (1976)	14.619
6	14168	$CuTeO_3$	Te2	Lindqvist (1972)	14.419
7	24781	$NaKTeO_3{\cdot}3H_2O$	Te1	Daniel *et al.* (1982)	23.739
8	25021	$Fe_2Te_4O_{11}$	Te2	Pertlik (1972)	14.267
9	26451	$Li_2Te_2O_5$ ($P2_1/n$)	Te2	Cachau-Herreillat *et al.* (1981)	14.484
10	26533	$NiTe_2O_5$	Te2	Platte & Trömel (1981)	13.763
11	26536	$Na_2Te_2O_5{\cdot}2H_2O$	Te2	Daniel *et al.* (1981)	18.036
12	27515	TeO_2 ($P4_12_12$)	Te1	Lindqvist (1968)	14.894
*13	35345	$K_2Te_2O_5{\cdot}3H_2O$	Te1	Andersen & Moret (1983)	10.337
14	36394	$In_2Te_3O_9$	Te1	Philippot *et al.* (1978)	14.473
15	37069	$Ba_3Te_4O_{11}$	Te3	Hottentot & Loopstra (1983)	19.903
16	48114	$MgTeO_3{\cdot}6H_2O$	Te1	Andersen *et al.* (1984)	18.568
17	50702	$Co_2Te_3O_8$	Te2	Feger *et al.* (1999)	12.763
18	50703	$Ni_2Te_3O_8$	Te2	Feger *et al.* (1999)	12.740
19	50704	$Cu_2Te_3O_8$	Te2	Feger *et al.* (1999)	12.949
20	50705	$Zn_2Te_3O_8$	Te2	Feger *et al.* (1999)	12.917
21	59167	$Cs_2Te_4O_9$	Te1	Loopstra & Goubitz (1986)	14.929
22	60067	$CdTeO_3$	Te2	Krämer & Brandt (1985)	12.246
23	61673	$HgTeO_3$	Te2	Krämer & Brandt (1986)	14.900
24	68878	$Nd_2Te_4O_{11}$	Te1	Castro *et al.* (1990)	14.789
*25	68878	$Nd_2Te_4O_{11}$	Te2	Castro *et al.* (1990)	12.261
26	73991	$MnTe_2O_5$	Te1	Miletich (1993)	11.932
*27	74396	$SrTeO_3$ ($P1$)	Te1	Elerman (1993)	12.757
*28	74396	$SrTeO_3$ ($P1$)	Te5	Elerman (1993)	12.463
29	82490	$Mn_2Te_3O_8$	Te2	Cooper & Hawthorne (1996)	13.359
30	82641	$Bi_2Te_2W_3O_{16}$	Te1	Champarnaud-Mesjard *et al.* (1996)	13.164
31	85922	$NaGaTe_2O_6$	Te1	Miletich & Pertlik (1998)	14.971
32	87978	$(NH_4)_4(Mo_6TeO_{22}){\cdot}2H_2O$	Te1	Balraj & Vidyasagar (1999)	11.663
33	87979	$Rb_4(Mo_6TeO_{22}){\cdot}2H_2O$	Te1	Balraj & Vidyasagar (1999)	11.564
*34	88996	$Sr_3Te_4O_{11}$	Te1	Dytyatev & Dolgikh (1999)	10.775
35	88996	$Sr_3Te_4O_{11}$	Te3	Dytyatev & Dolgikh (1999)	15.872
36	88996	$Sr_3Te_4O_{11}$	Te6	Dytyatev & Dolgikh (1999)	17.961
*37	88996	$Sr_3Te_4O_{11}$	Te7	Dytyatev & Dolgikh (1999)	13.256
38	89893	$CaCu_{10}(TeO_3)_4(AsO_4)_2(OH)_2{\cdot}4H_2O$	Te1	Burns *et al.* (2000)	13.752
39	89893	$CaCu_{10}(TeO_3)_4(AsO_4)_2(OH)_2{\cdot}4H_2O$	Te2	Burns *et al.* (2000)	14.155
40	90109	$Rb_2TeMo_2O_6(PO_4)_2$	Te1	Guesdon & Raveau (2000)	13.130

vertices. Volumes of the $Te^{IV}O_6$ polyhedra were calculated in the visualization software package *CrystalMaker*® (CrystalMaker Software Ltd, Oxford, UK; http://www.crystalmaker.com). The range of volumes of these polyhedra was extraordinarily wide, from 10.3 to 23.7 Å^3, or 80 to 185% of the volume of a regular $Te^{IV}O_6$ polyhedron. In one case ($Sr_3Te_4O_{11}$; Dytyatev & Dolgikh, 1999), four symmetrically distinct TeO_6 polyhedra have volumes between 10.78 and 17.96 Å^3 in the same structure. Clearly, distortion associated with lone-pair stereoactivity can cause either moderate contraction or very strong expansion of the polyhedron, so it is an oversimplification to assume that increasing distortion always leads to expansion.

Our aim in this study was to survey a range of different measures of polyhedral distortion, in order to identify which of them best displayed the properties expected for the 'degree of lone-pair stereoactivity', how that property correlated with polyhedral volume, and which were the other principal factors involved in controlling the volume of the polyhedron.

2.1. Measures of polyhedral distortion

Before we can quantify distortion, an 'undistorted' reference state must be defined; as mentioned above, this is the regular octahedron with ideal bond lengths for this study. Polyhedra have a large number of degrees of freedom (the shape of a general MX_6 group requires 15 parameters for full description, corresponding to the 7×3 independent coordinates of the constituent atoms minus 6 rigid-body rotations and translations). Rather than work in such a multi-dimensional parameter space, authors have devised many approaches to represent distortion as a single or small number of parameters. The simplest possibility, arising directly from the Distortion Theorem, is the mean bond distance. The distortion theorem implies that this should correlate strongly with the variance of bond distances. The mean bond distance is equivalent, less a subtracted constant, to the deviation of the mean bond distance from the ideal bond distance in the regular polyhedron, as advocated by Brown (2006), who compared this parameter with the distortion parameter of Lalik (2005), which is founded in information theory, but is in essence a bond-valence weighted mean bond distance. Urusov (2006) showed that bond-distance variance correlates with mean bond distance, but that the quantitative relationship varies with the style of distortion. Another pair of quite different distortion parameters that show mutual correlation are bond-angle variance and 'quadratic elongation', defined as the mean-squared ratio of bond distances to the distance in a regular polyhedron of the same volume, but not necessarily with the ideal bond-valence sum at the central atom (Robinson *et al.*, 1970). A problem noted by Brown (2006) is that most distortion measures assume that all ligands have the same identity, and cannot be applied where this is not the case. A relatively recent approach that solves this problem is the use of the vectorial bond-valence sum of Harvey *et al.* (2006). This allows robust determination of the most symmetrical point in any coordination polyhedron and provides a coupling between bond-distance distortion and angular distortion in polyhedra

Table 2
Parameters for TeO_6 polyhedra of this study.

Symbols are: $\langle r\rangle$ = mean bond distance, $\sigma(r)$ = standard deviation of bond distances, $|\mathbf{S}|$ = magnitude of vector bond valence, C_{poly} = geometrical centroid of O_6 polyhedron, Δ = distance from Te to centre C_{sph} of O_6 sphere of best fit, R_{sph} = radius of sphere, σ_{sph} = standard deviation of O—C_{sph} distances.

	$\langle r\rangle$ (Å)	$\sigma(r)$ (Å)	$\lvert\mathbf{S}\rvert$ (v.u.)	Te—C_{poly} (Å)	Δ (Å)	R_{sph} (Å)	σ_{sph} (Å)
1	2.377	0.567	1.822	0.369	1.084	2.602	0.097
2	2.487	0.653	1.479	0.570	1.061	2.575	0.166
3	2.451	0.621	1.609	0.408	0.959	2.561	0.147
4	2.436	0.662	1.738	1.148	1.203	2.689	0.058
5	2.413	0.625	1.828	0.624	1.126	2.618	0.106
6	2.394	0.617	1.607	0.510	1.179	2.648	0.145
7	2.363	0.579	1.808	0.517	1.648	2.962	0.000
8	2.270	0.501	1.868	0.545	0.786	2.406	0.038
9	2.475	0.775	1.683	0.374	1.035	2.561	0.162
10	2.575	0.789	1.512	0.379	0.767	2.399	0.118
11	2.304	0.447	1.781	0.234	1.355	2.808	0.110
12	2.672	0.891	1.486	0.057	0.881	2.469	0.099
*13	2.317	0.509	1.647	0.658	1.322	2.768	0.120
14	2.305	0.483	1.622	0	0.936	2.514	0.074
15	2.329	0.533	1.778	0.395	1.516	2.911	0.047
16	2.327	0.533	1.797	1.068	1.104	2.581	0.000
17	2.390	0.610	1.761	0.352	1.029	2.618	0.124
18	2.322	0.469	1.698	0.347	0.958	2.573	0.127
19	2.395	0.619	1.741	0.402	1.033	2.607	0.117
20	2.640	0.851	1.805	0.366	1.075	2.644	0.124
21	2.426	0.632	1.602	0.211	1.303	2.751	0.226
22	2.346	0.547	1.773	0.292	1.444	2.934	0.253
23	2.334	0.516	1.690	0.022	0.996	2.565	0.048
24	2.660	0.908	1.681	0.164	1.706	3.077	0.217
*25	2.290	0.468	1.640	0.706	0.939	2.498	0.190
26	2.476	0.744	1.741	0.315	1.103	2.644	0.074
*27	2.476	0.697	2.042	0.930	1.168	2.697	0.363
*28	2.438	0.664	1.966	1.010	1.242	2.743	0.085
29	2.319	0.500	1.779	0.334	1.092	2.659	0.109
30	2.345	0.536	1.767	0.323	0.907	2.507	0.051
31	2.308	0.480	1.730	0.446	0.854	2.467	0.083
32	2.241	0.382	1.567	0.102	0.831	2.449	0.073
33	2.241	0.379	1.581	0.109	0.837	2.454	0.062
*34	2.548	0.746	1.719	0.902	1.441	2.889	0.129
35	2.450	0.688	1.900	0.266	1.472	2.886	0.170
36	2.511	0.755	1.756	0.794	1.456	2.830	0.121
*37	2.502	0.704	1.678	0.706	1.248	2.725	0.095
38	2.354	0.511	1.737	0.381	1.043	2.619	0.031
39	2.424	0.634	1.834	0.456	1.431	2.884	0.060
40	2.333	0.548	1.765	0.146	1.304	2.784	0.164

(Brown, 2013*b*), and correlates in magnitude with distortion measures related to the shortest bond distance (Bickmore *et al.*, 2013). Many other simple distortion measures are referenced by Urusov (2003) and Brown (2006).

We examined several distortion parameters for possible correlation with polyhedral volume, and in most cases found little or no relationship. However, some distortion measures which did yield evocative results were those of Balić-Žunić & Makovicky (1996) and Makovicky & Balić-Žunić (1998). These authors sought a description of distortion that was independent of the geometry and topology peculiar to any specific polyhedron, and hence defined a sphere of best fit to the shell of ligands. The deviation of a polyhedron from ideal could then be quantified in terms of:

(i) the radius R_{sph} of the sphere of best fit (relative to that for a regular polyhedron);

(ii) the standard deviation σ_R of distances from ligands to the surface of that sphere, and the derived quantity 'sphericity' $= 1 - \sigma_R/R_{sph}$;

(iii) the distance Δ from the central atom to the centre of the sphere;

(iv) Makovicky & Balić-Žunić (1998) also introduced a volume distortion parameter which is the proportionate difference between the volume V_{poly} of a distorted polyhedron and the volume V_{reg} of a regular polyhedron with the same sphere of best fit, $\upsilon\% = 100 \times (V_{reg} - V_{poly})/V_{reg}$.

The results presented below make use of these parameters and others closely related to them.

3. Results

We first plotted the mean bond distance $\langle r\rangle$ against the standard deviation $\sigma(r)$ of bond distances for the polyhedra of this study. The data are shown in Table 2. There was a strong covariation, as anticipated from the distortion theorem. This appeared to be approximately linear, except that it did not extrapolate to $r = 2.127$ Å at $\sigma(r) = 0$, as would be expected from the bond-valence parameters of Mills & Christy (2013). A quadratic fit extrapolated much closer to that value (< 0.04 Å) than either a linear or cubic fit, and also had a slightly improved regression coefficient for fitted against observed values

$$\langle r\rangle = 2.089 + 0.2283\sigma(r) + 0.460\sigma^2(r) \quad (r^2 = 0.957). \qquad (2)$$

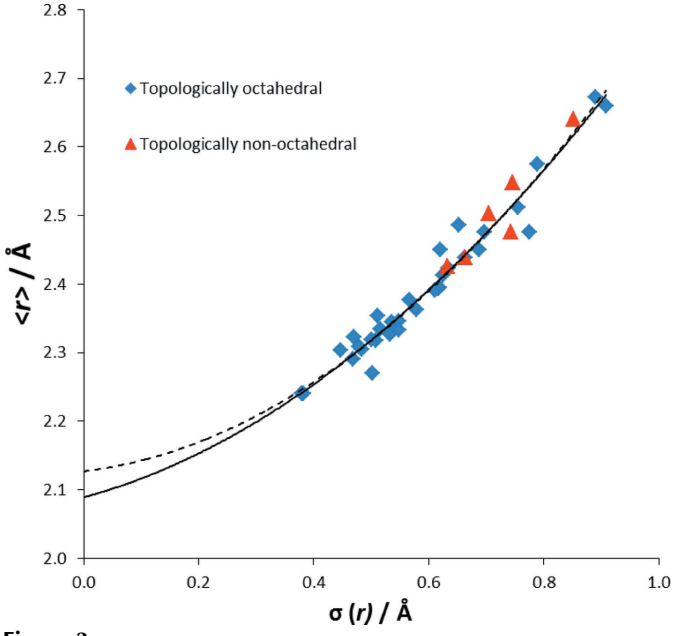

Figure 3
Mean bond distance $\langle r\rangle$ for $Te^{IV}O_6$ polyhedra of this study, plotted against standard deviation $\sigma(r)$. Fitted curves are unconstrained quadratic (solid line) and quadratic constrained to pass through $\langle r\rangle = 2.127$ Å at $\sigma(r) = 0$ (dashed line), consistent with the Te^{IV}—O bond-valence parameters of Mills & Christy (2013).

Table 3
Parameters relating to the filling of the sphere of best fit by a polyhedron.

Polyhedral volume is repeated from Table 1 for convenience. Other symbols: r_{C-C} = distance between C_{poly} and C_{sph}, $\zeta = r_{C-C}/R_{sph}$, V_{calc} = volume estimated from Δ and r_{C-C} using the regression equations in the text.

	r_{C-C} (Å)	ζ	$1-\zeta^2$	V_{poly} (Å^3)	V_{sph} (Å^3)	V_{poly}/V_{sph}	V_{calc} (Å^3)
1	0.999	0.384	0.853	14.338	73.809	0.194	15.083
2	0.662	0.257	0.934	16.028	71.494	0.224	17.608
3	0.646	0.252	0.936	15.882	70.342	0.226	16.316
4	1.056	0.393	0.846	16.169	81.408	0.199	16.261
5	1.053	0.402	0.838	14.619	75.188	0.194	15.063
6	1.115	0.421	0.823	14.419	77.811	0.185	15.102
7	1.131	0.382	0.854	23.739	108.832	0.218	22.813
8	0.646	0.268	0.928	14.267	58.356	0.244	13.915
9	0.926	0.362	0.869	14.484	70.350	0.206	15.074
10	0.740	0.308	0.905	13.763	57.848	0.238	13.069
11	1.150	0.410	0.832	18.036	92.753	0.194	17.625
12	0.824	0.334	0.889	14.894	63.022	0.236	13.891
*13	1.230	0.444	0.803	10.337	88.816	0.116	15.957
14	0.924	0.368	0.865	14.473	66.564	0.217	13.792
15	1.217	0.418	0.825	19.903	103.317	0.193	19.431
16	0.036	0.014	1.000	18.568	72.028	0.258	20.552
17	1.186	0.453	0.795	12.763	75.170	0.170	12.507
18	1.119	0.435	0.811	12.740	71.386	0.178	12.329
19	1.144	0.439	0.807	12.949	74.184	0.175	12.970
20	1.218	0.461	0.788	12.917	77.380	0.167	12.721
21	1.265	0.460	0.789	14.929	87.199	0.171	15.158
22	1.647	0.561	0.685	12.246	105.774	0.116	12.042
23	1.001	0.390	0.848	14.900	70.647	0.211	13.909
24	1.731	0.563	0.683	14.789	121.996	0.121	14.358
*25	0.676	0.271	0.927	12.261	65.277	0.188	15.755
26	1.229	0.465	0.784	11.932	77.424	0.154	12.867
*27	0.820	0.304	0.908	12.757	82.128	0.155	18.142
*28	1.222	0.446	0.801	12.463	86.403	0.144	14.997
29	1.205	0.453	0.795	13.359	78.740	0.170	13.134
30	0.797	0.318	0.899	13.164	65.962	0.200	14.503
31	0.793	0.322	0.897	14.971	62.854	0.238	13.819
32	0.933	0.381	0.855	11.663	61.548	0.189	12.365
33	0.947	0.386	0.851	11.564	61.888	0.187	12.317
*34	1.483	0.513	0.736	10.775	100.971	0.107	14.373
35	1.424	0.493	0.757	15.872	100.688	0.158	15.632
36	1.191	0.421	0.823	17.961	94.960	0.189	18.520
*37	1.121	0.411	0.831	13.256	84.759	0.156	16.227
38	1.116	0.426	0.818	13.752	75.214	0.183	13.445
39	1.523	0.528	0.721	14.155	100.489	0.141	13.577
40	1.450	0.521	0.729	13.130	90.404	0.145	12.697

However, a quadratic fit that was contrained to pass through the y axis at $\langle r\rangle$ = 2.127 Å had almost the identical regression coefficient and was visually coincident with the other curve where it passed through the data points

$$\langle r\rangle = 2.127 + 0.1004\sigma(r) + 0.5632\sigma^2(r) \quad (r^2 = 0.957). \quad (3)$$

The fitted curves are shown in Fig. 3. Note that the figure distinguishes by different symbols two subsets of the data. Although these follow the same trend in Fig. 3, the six 'non-octahedral' polyhedra were outliers on many other charts made during this study. Close inspection of the actual coordination polyhedra in the structures revealed that these were not topologically octahedral. A polyhedron has the same topology as a regular octahedron if four edges meet at each of the six vertices. However, these six polyhedra were so deformed that two vertices had edges running to all five of the others, giving the overall form of a pentagonal pyramid with a slightly nonplanar base (Fig. 4). The pyramidal polyhedra are indicated by asterisks in Tables 1–3.

Polyhedral volume is plotted against mean $Te^{IV}-O$ distance in Fig. 5. If non-octahedra were not distinguished, the data would appear to spread over a triangular field. However, when topologies were distinguished as in Fig. 3, it became apparent that the data for true octahedra lay on a positive linear trend. Because of the considerable scatter, the low correlation coefficient (r^2 = 0.75) did not increase if other polynomial fits were applied.

The vector bond valence of Harvey *et al.* (2006) was calculated for all the polyhedra of this study, and was always significant in magnitude: 1.47–2.04 valence units (v.u.). It showed a negligible correlation with mean bond distance (r^2 = 0.11) or polyhedral volume (r^2 = 0.04) and only weak trends when plotted against the maximum bond valence and minimum coordination number parameters of Bickmore *et al.* (2013). For reference, the magnitude of vector bond valence has been included in Table 2. The modified vector bond valence of Zachara (2007) was also calculated, but correlated even worse with other parameters than the original version; this was not considered further.

The off-centring of the Te^{IV} atom from the centre of the O_6 polyhedron would be expected to correlate strongly with lone-pair stereoactivity. The geometrical centroid C_{poly} of the polyhedron was defined by the mean of the position vectors of the six O atoms. The sum of squares of distances from the centre to the O atoms is minimized at this point. The distance

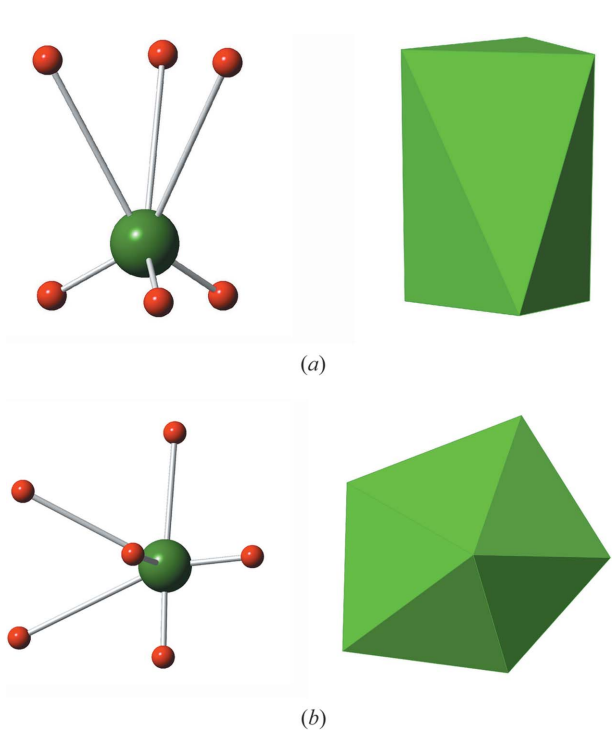

Figure 4
(*a*) Ball-and-stick and polyhedral views of the $Te^{IV}O_6$ polyhedron of $MgTeO_3{\cdot}6H_2O$ (Table 1, #16), showing stretched octahedral shape with trigonal symmetry. (*b*) Polyhedron surrounding Te1 of $Sr_3Te_4O_{11}$ (Table 1, #34), showing approximate pentagonal pyramidal shape with five edges converging at one vertex.

of Te^{IV} from this position, calculated in *CrystalMaker*®, was 0–1.15 Å, with a mean of 0.45 Å and standard deviation 0.29 Å. Surprisingly, no correlation was observed between the Te—C_{poly} distance and polyhedron volume (r^2 = −0.01) or Te—C_{poly} distance and vector bond valence (r^2 = 0.00).

An alternative method of identifying a centre for the polyhedron is as the centre of a sphere of best fit for the O atoms. At this point C_{sph}, the variance of distances to the O atoms is minimized. The algorithm for calculating this position is given by Balić-Žunić & Makovicky (1996). The distance Δ of Te^{IV} to C_{sph} is larger than the Te—C_{poly} distance, with the range 0.76–1.71 Å, mean 1.15 Å and a smaller standard deviation of 0.24 Å. This distance Δ is more consistent with the cation–lone pair distances of Hyde & Andersson (1989), who model the lone pair as a quasi-anion (*cf.* Figs. 2*a* and *b*). They give 1.25 Å as a typical cation–lone-pair distance for Te^{IV}.

The standard deviations σ_{sph} of distances C_{sph}—O for polyhedra were small. The ratios (σ_{sph}/R_{sph}), where R_{sph} is the fitted sphere radius, was 0–0.135, with a mean value of 0.043 for the 40 polyhedra. By considering the change to a tetrahedral volume element defined by three O atoms and C_{sph}, if one C_{sph}—O distance is increased by a small amount (δ) and another is decreased by the same amount, it is readily shown that the volume varies proportional to $(1 - \delta^2)$, and hence that the volume of the whole polyhedron varies according to $1 - (\sigma_{sph}/R_{sph})^2$. Hence, departure from sphericity does not perturb the volume of the polyhedra of this study by more than 2%, and more typically does so by only 0.2%. Thus, the O atoms do indeed lie on the surface of a sphere to a very good approximation. This lends credence to the idea that the anions maintain a nearly constant distance from an entity at the sphere centre, which can be equated with the lone pair.

No correlation was observed between the two types of Te—*C* distance (r^2 = 0.08), or between Δ and vector bond valence (r^2 = 0.17). The Te^{IV}—C_{sph} distance Δ showed a positive correlation with $\langle r \rangle$, albeit with considerable scatter (r^2 = 0.48). This is as expected if Δ represents the degree of lone-pair stereoactivity, while the mean Te^{IV}—O distance increases with polyhedral distortion in accordance with the distortion theorem. No significant correlation was seen between Δ and the polyhedral volume V_{poly} (r^2 = 0.15). However, a very strong linear correlation was found between Δ and R_{sph} (Fig. 6). For the true octahedra

$$R_{sph} = 1.883 + 0.6809\Delta \quad (r^2 = 0.975). \qquad (4)$$

The pyramidal polyhedra also lie along the same trend, suggesting that this relationship is not sensitive to polyhedral topology. The Te—C distances and sphere parameters R_{sph} and σ_{sph} are given in Table 2. The extremely strong correlation of equation (4) further supports the notion that the sphere of best fit and the location of its centre are physically significant. This relationship arises presumably because the greater stereoactivity of the lone pair (measured by Δ, corresponding to the distance between cations and quasi-anions in Fig. 2*a*) is reflected in greater non-bonded electron density at the sphere centre (identified with the centroids of the lone-pair caps of Fig. 2*b*) and hence greater repulsion between that non-bonding density and the anions of the polyhedron. Increasing Δ thus increases the non-bonded distance between anions and the lone pair, at which this repulsion is balanced by the attractive force mediated through the bonds to the central

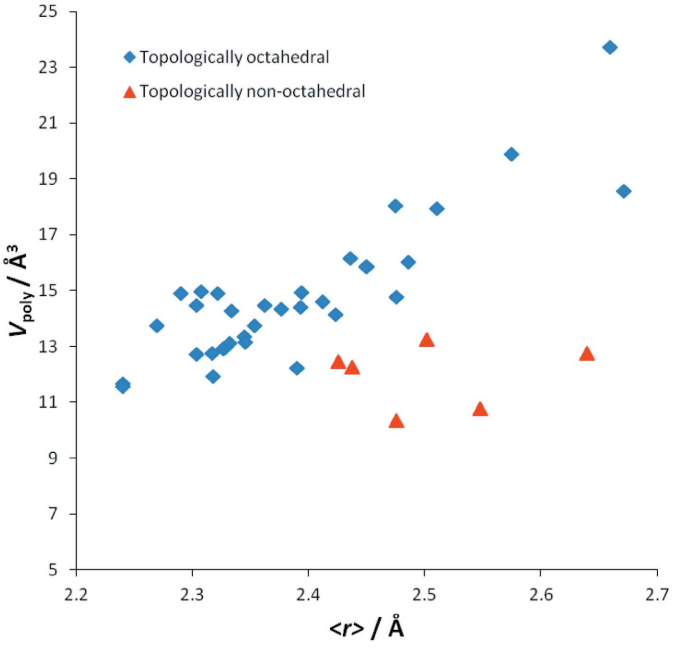

Figure 5
Polyhedral volume *versus* mean bond distance, showing the trend with some scatter for topological octahedra, while non-octahedra are low-volume outliers.

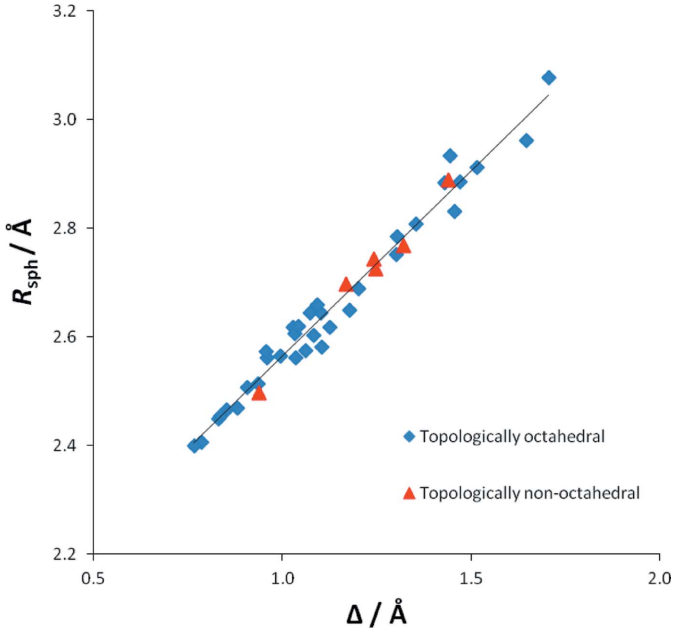

Figure 6
Well defined linear relationship between the Te—C_{sph} distance Δ and sphere radius, irrespective of polyhedral topology.

cation. There is sufficient flexibility in placement of the anions on the surface of the sphere that although the mean Te^{IV}—O distance $\langle r \rangle$ and R_{sph} correlate positively, they do so weakly ($r^2 = 0.38$). It is clear that the well defined linear relationship of equation (4) and Fig. 6 is not predominantly a consequence of the overall increase in mean bond distance with distortion.

Despite their importance as indicators of lone-pair stereoactivity and lone pair–anion interaction, the parameters Δ and R_{sph} are poor predictors of polyhedral volume V_{poly}. A plot of V_{poly} against R_{sph} showed $r^2 = 0.29$. This is because the behaviour of V_{poly} is affected by an additional aspect of polyhedral geometry that is highly variable, namely the extent to which the O_6 polyhedron fills the sphere. Fig. 7 shows again the polyhedra of Fig. 4, with their respective spheres of best fit. The $MgTeO_3{\cdot}6H_2O$ polyhedron is a slightly stretched octahedron with trigonal symmetry (Andersen *et al.*, 1984). It is appreciably larger than the ideal regular $Te^{IV}O_6$ octahedron ($V_{poly} = 18.57$ Å^3, compared with 12.83 Å^3), has a moderately large sphere [$R_{sph} = 2.581$ Å, $V_{sph} = (4/3)\pi R_{sph}^3 = 72.03$ Å^3], but O atoms are distributed across both the top and bottom halves of the sphere and the polyhedron occupies a relatively large proportion of the spherical space: $V_{poly}/V_{sph} = 0.258$. The most uniform distribution of O atoms, forming a regular octahedron circumscribed by the sphere, would have $V_{poly}/V_{sph} = 1/\pi \simeq 0.318$. Conversely, the very flattened pyramidal polyhedron of $Sr_3Te_4O_{11}$ Te1 (Dytyatev & Dolgikh, 1999) has all its O atoms confined to a small portion of a very inflated sphere. In this case, $R_{sph} = 2.889$ Å, $V_{sph} = 100.97$ Å^3, but V_{poly} is only 10.78 Å^3, because V_{poly}/V_{sph} takes the much lower value of 0.107. The polyhedra depicted exhibit the extreme values of V_{poly}/V_{sph} for this study; all others have intermediate values. The ratio V_{poly}/V_{sph} is closely related to the volume defect parameter υ % of Makovicky & Balić-Žunić (1998): $\upsilon = 100 \times (1 - \pi V_{poly}/V_{sph})$, if the reference polyhedron is a regular octahedron.

It is apparent from Fig. 7 that the centroid C_{poly} of the O_6 polyhedron lies very close (0.036 Å) to the centre of the sphere C_{sph} for $MgTeO_3{\cdot}6H_2O$, while the two centres are well separated (1.483 Å) for $Sr_3Te_4O_{11}$ Te1. If the two centres coincide, then the O atoms are rather uniformly distributed over the sphere, and the coordination polyhedron can occupy much of the width of the sphere. Conversely, as C_{poly} moves further away from the centre of the sphere, the polyhedron is

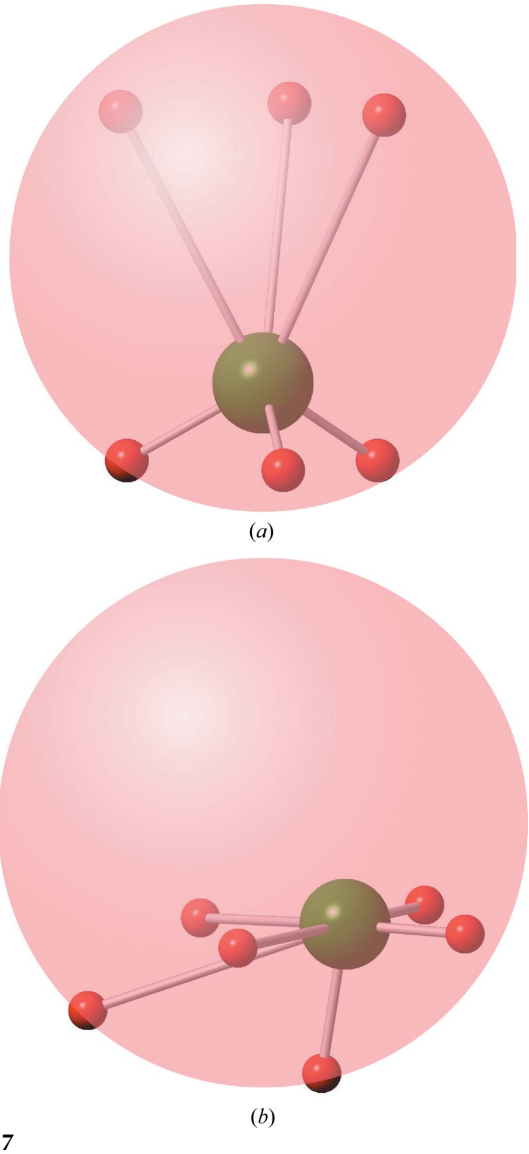

Figure 7
The polyhedra of Fig. 4, shown inside their spheres of best fit. (*a*) Topologically octahedral $Te^{IV}O_6$ of $MgTeO_3{\cdot}6H_2O$, with O atoms spanning much of the sphere. The centroid of the polyhedron nearly coincides with that of the sphere: $r_{C-C} = 0.036$ Å. The polyhedron is relatively large ($V_{poly} = 18.57$ Å^3) because it occupies a large fraction of a small sphere ($R_{sph} = 2.581$ Å, $V_{sph} = 72.03$ Å^3, $V_{poly}/V_{sph} = 0.258$). (*b*) Pyramidal $Te^{IV}O_6$ of $Sr_3Te_4O_{11}$ Te1, with O atoms confined to one side of the sphere. The centroid of the polyhedron and the sphere centre are far apart: $r_{C-C} = 1.483$ Å. The polyhedron is small ($V_{poly} = 10.78$ Å^3) because it occupies a very small fraction of a large sphere ($R_{sph} = 2.889$ Å, $V_{sph} = 100.97$ Å^3, $V_{poly}/V_{sph} = 0.107$).

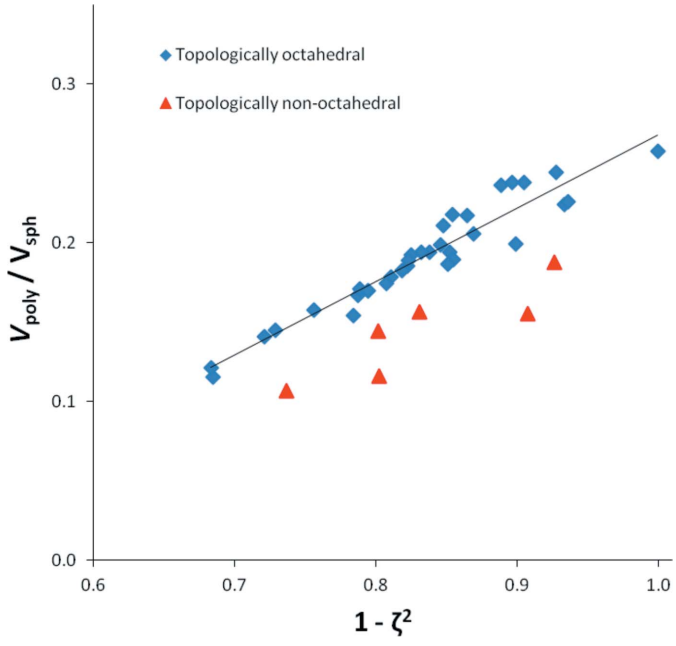

Figure 8
Correlation for octahedra between the degree of filling of the sphere of best fit and the parameter ζ, derived in the text from the distance between sphere centre and polyhedron centroid.

confined to smaller segments of the sphere, and the cross-sectional area of the polyhedron becomes restricted to correspondingly smaller values. This suggests that the distance r_{C-C} between C_{poly} and C_{sph} can be used to estimate V_{poly}/V_{sph}. If we define $\zeta = r_{C-C}/R_{sph}$, the maximum possible cross-section would be expected to decrease roughly proportional to $(1 - \zeta^2)$. A good linear relationship can be seen in Fig. 8 between $(1 - \zeta^2)$ and (V_{poly}/V_{sph}) for the topological octahedra

$$(V_{poly}/V_{sph}) = 0.464(1 - \zeta^2) - 0.1957 \quad (r^2 = 0.916). \qquad (5)$$

The remaining six polyhedra appear to lie on a separate but parallel trend, with smaller volumes.

We have established that the offset Δ between the central cation and the sphere centre quantifies the degree of lone-pair stereoactivity, and that a strong correlation exists between Δ and R_{sph}. Thus, the degree of lone-pair activity determines the size of the spherical surface on which the anions are distributed. However, the distribution of anions around the sphere can vary quite independently of Δ, and the asymmetry of this is approximately measured by polyhedron centroid–sphere centre distance r_{C-C}. This determines the efficiency with which the polyhedron fills the sphere, giving another strong correlation between r_{C-C} and V_{poly}/V_{sph}. Putting equations (4) and (5) together, we can obtain an estimate for the polyhedral volume, derived from Δ and r_{C-C}. The resulting V_{calc} values are compared with the experimental volumes V_{poly} in Fig. 9. For true octahedra, a linear relationship is obtained, with a gradient close to unity and intercept close to zero

$$V_{calc} = 0.9704V_{poly} + 0.4711 \quad (r^2 = 0.912). \qquad (6)$$

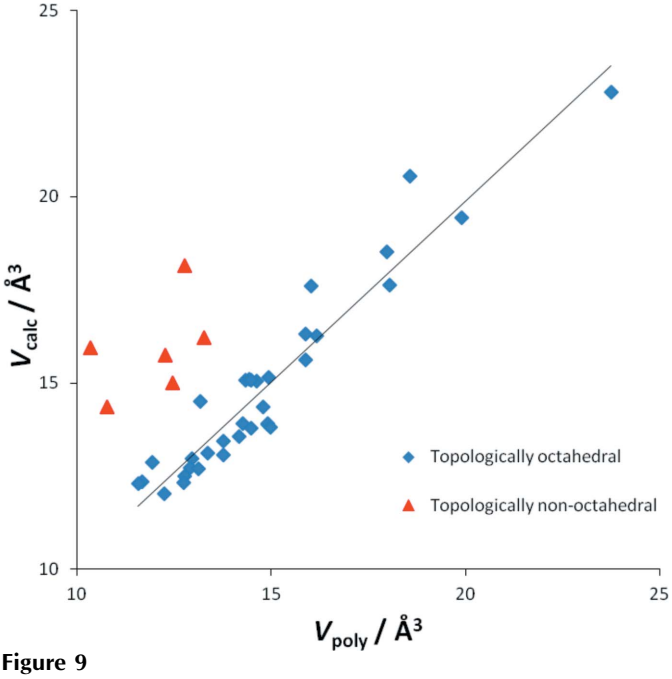

Figure 9
Experimental volumes of polyhedra V_{poly} compared with those calculated from just Δ and r_{C-C}.

The r.m.s. deviation between V_{calc} and V_{poly} is 0.75 Å^3, or about 3–7%. Thus, about 95% of the variation in V_{poly} can be accounted for as a function of just the two parameters Δ and r_{C-C}. Much of the remaining deviation may be due to inaccuracies or intrinsic strain in the determined structures. However, equation (6) applies only for polyhedra that are topologically octahedral. The pyramidal polyhedra form a separate cluster in Fig. 9, with volumes much smaller than would be predicted by this equation. While relationships such as those of equations (5)–(6) may exist for a wide range of polyhedra, the numerical coefficients differ for different polyhedral topologies. The parameters r_{C-C}, ζ and calculated polyhedral volumes V_{calc} are given in Table 3.

4. Conclusions

Although the mean bond distance increases with the irregularity of a coordination polyhedron in accordance with the Distortion Theorem, this does not always imply that the volume of the polyhedron increases. The 40 $Te^{IV}O_6$ polyhedra of this study show a very wide range of volumes, from 80–185% of the 12.83 Å^3 predicted for the regular $Te^{IV}O_6$ octahedron using the bond-valence parameters of Mills & Christy (2013).

Most measures of polyhedral distortion described in the literature (quadratic elongation, bond-angle variance, vector bond valence *etc.*) do not correlate well with polyhedral volume. However, we have found relationships for $Te^{IV}O_6$ polyhedra with octahedral topology that allow volume to be predicted with good accuracy from just two parameters. The nature of these parameters demonstrates that fitting a sphere of best fit to the ligand shell, as advocated by Balić-Žunić & Makovicky (1996) and Makovicky & Balić-Žunić (1998), has considerable physical significance. The O atoms of all our polyhedra lie close to a spherical surface, whether the polyhedron is of octahedral topology or not. The centre of the sphere lies 0.7–1.7 Å from the central cation, at the distance expected for a stereoactive lone pair in the model of Hyde & Andersson (1989). The radius of the sphere R_{sph} is a linear function of the offset Δ of the central cation from the sphere centre, irrespective of polyhedral topology.

This relationship is explained as a result of increased repulsion between the anions and the greater non-bonding electron density as a lone pair becomes more localized, which leads to an increase in non-bonded distance between the lone pair and the anions.

However, the O atoms may span a large or small portion of the spherical surface area, quite independent of the radius of their sphere of best fit, and this is what allows the extraordinary variability of polyhedral volume. An approximate measure of the degree to which the polyhedron fills the sphere can be derived from the distance between the sphere centre and the centroid of the O atoms. For octahedra, an equation can be written that predicts volume to within a few percent using just the centroid–centre distance r_{C-C} and Δ. Similar relationships probably occur for other types of polyhedron, albeit with different numerical coefficients in the equations.

The six polyhedra that have coordination approximating pentagonal pyramidal rather than octahedral show the same relationships as octahedra for mean *versus* standard deviation of bond distance and for Δ *versus* sphere radius, but otherwise are low-volume outliers. The sphere centre C_{sph} lies well outside the O_6 polyhedron in these cases, as can be seen from the example in Fig. 6. This can be interpreted as the lone pair pointing into a void in the anion substructure; there are no further O atoms within 4 Å of the Te^{IV} cation. However, in all cases, there are multiple additional Te^{IV} cations and/or large, polarizable cations (K^{I}, Sr^{II}, Nd^{III}) at 3.3–4 Å on this side of the central Te^{IV} atom. Bonding between such a species (Na^{I}) and the lone pair of Sn^{II} is discussed in the case of Na_4SnO_3 by Brown (2011). Thus, in the non-octahedral polyhedra of this study, weak bonds occur between lone pairs and large, deformable cations and/or attractive dipole–dipole interactions occur between lone-pair cations, and that the full coordination sphere around the central lone pair should include these additional non-anionic species. These cases provide extreme examples of the responsivity of lone-pair coordination polyhedra to the local environment. It is very frequently the case that two topologically similar but symmetrically distinct coordination polyhedra in the same structure may show quite different degrees of lone-pair activity Δ, polyhedron-sphere asymmetry ζ and polyhedron volume. This is well demonstrated by the two distorted $Te^{IV}O_6$ octahedra of juabite, $CaCu_{10}(TeO_3)_4(AsO_4)_2(OH)_2{\cdot}4H_2O$ (Burns *et al.*, 2000), which are numbers 38–39 in Tables 1–3 of this study. Quite different oxygen coordination numbers can also occur: for balyakinite, $CuTeO_3$ (Lindqvist, 1972), Te1 has 9 oxygen neighbours (Fig. 1), while Te2 has only 6 (Tables 1–3, #6).

The flexibility of volume displayed by the lone-pair coordination polyhedra means that polyhedra cannot be assumed to become more symmetrical with the application of pressure. Contraction of polyhedra can be achieved by making the ligand geometry less symmetrical, even if the sphere of best fit increases in radius (which is our measure of increasing lone-pair stereoactivity). Furthermore, the polyhedron is free to expand with pressure, if other parts of the structure can contract sufficiently to compensate. Symmetrization of polyhedra due to decrease in lone-pair activity with increasing pressure is well documented for compounds such as stibnite, Sb_2S_3, and bismuthinite, Bi_2S_3 (Lundegaard *et al.*, 2003, 2005). However, high-pressure experiments show that some lone-pair materials behave in the opposite fashion. For example, transformations to structures with lone-pair cations in *less* regular coordination environments with increasing pressure are known for PbO (Adams *et al.*, 1992), PbS (Grzechnik & Friese, 2010), and the sulfosalts $Pb_3Bi_2S_6$ and $Pb_6Bi_2S_9$ (Olsen *et al.*, 2008, 2011).

Conversely, for a given geometry of ligands, it is possible for bond valences to be equally satisfied either for a large cation with relatively little lone-pair stereoactivy, or for a smaller cation with a more active lone pair. This suggests that solid solutions between lone-pair cations can be unusually flexible, and there is evidence that this is so. Consider $Pb^{II}-O$ and $Te^{IV}-O$, which for the case of hypothetical regular MO_6 octahedra are estimated to have bond distances of 2.469 and 2.127 Å using the bond-valence parameters of Krivovichev & Brown (2001) and Mills & Christy (2013), respectively. Note that the formal charges on Pb and Te differ by 2 v.u., and also that the $Pb^{II}-O$ distances are $\sim$16% longer than $Te^{IV}-O$ distances, corresponding to a 47% difference in traditional ionic radii if $r_{O^{2-}} = 1.40$ Å is assumed. Both of these differences would make extensive solid solution unlikely according to Goldschmidt's Rules (Goldschmidt, 1926), which would favour solid solution only if the charge difference is 1 v.u. or less and the ionic radius difference is < 15%. Nevertheless, Kampf *et al.* (2010) described the mineral telluroperite, $Pb^{II}_3Te^{IV}O_4Cl_2$ and published a single-crystal structure refinement for it, in which equal proportions of Pb^{II} and Te^{IV} mix randomly on one cation site, bonded to 4O + 4Cl. They noted that the overall bond-valence sum for this cation was significantly low (2.42 rather than 3), and attributed the discrepancy to the average cation position being less off-centre than would be expected for Te^{IV}. Site splitting between the Pb^{II} and Te^{IV} locations is also supported by the large U^{33} displacement parameter for this site (Kampf *et al.*, 2010, Table 3). This is exactly what one would expect if the larger Pb^{II} sits closer to the polyhedron centre, with more equal bond distances and smaller Δ than the smaller Te^{IV}. Using the bond-valence parameters of Krivovichev & Brown (2001) for $Pb^{II}-O$, Brese & O'Keeffe (1991) for $Pb^{II}-Cl$, and Mills & Christy (2013) for $Te^{IV}-O$ and $Te^{IV}-Cl$, it is possible to estimate the separation between Pb^{II} and Te^{IV} by adjusting their z coordinates in order to obtain ideal bond-valence sums on both cations. The BVS equals the formal valence if $z = 0.044$ for Te^{IV} or $z = 0.139$ for Pb^{II}; these positions are 1.185 Å apart. The average z coordinate weighted by atomic number ($\sim$ scattering factor) is 0.102, close to the value of 0.0961 refined for the unsplit cation by Kampf *et al.* (2010). The calculated split is much larger that those observed when lone-pair cations substitute for large cations without stereoactive lone pairs, such as the 0.49–0.53 Å separation between the split Ba and Pb sites of hyalotekite (Christy *et al.*, 1998).

Overall, this study shows that the degree of stereoactivity of a lone pair on a central cation does not have a predictable effect on the volume of the surrounding coordination polyhedron. What is predictable is that the anions surround the lone pair at a non-bonded distance which increases with the the degree of stereoactivity. However, there is great flexibility in positioning of the anions within that shell surrounding the lone pair, which allows the coordination polyhedron to adopt a huge range of bonding patterns, volumes and geometries so as to fit the surrounding structure. The flexibility of lone-pair polyhedra is further enhanced by the ability of a single polyhedron to accommodate different cations with different degrees of lone-pair activity, which facilitates a broader range of solid solution than would otherwise be the case.

Part of this study has been funded by The Ian Potter Foundation grant 'tracking tellurium' to SJM which we gratefully acknowledge. We thank two reviewers for their very

thought-provoking comments, which have improved this manuscript.

References

Adams, D. M., Christy, A. G., Haines, J. & Clark, S. M. (1992). *Phys. Rev. B*, **46**, 11358–11367.
Alcock, N. W., Culver, J. & Roe, S. M. (1992). *J. Chem. Soc. Dalton Trans.* pp. 1477–1484.
Alcock, N. W. & Harrison, W. D. (1982). *Acta Cryst.* B**38**, 1809–1811.
Allmann, R. (1975). *Monatsh. Chem.* **106**, 779–793.
Andersen, L., Lindqvist, O. & Moret, J. (1984). *Acta Cryst.* C**40**, 586–589.
Andersen, L. & Moret, J. (1983). *Acta Cryst.* C**39**, 143–145.
Astier, R., Philippot, E., Moret, J. & Maurin, M. (1976). *Rev. Chim. Miner.* **13**, 359–372.
Balić-Žunić, T. & Makovicky, E. (1996). *Acta Cryst.* B**52**, 78–81.
Balraj, V. & Vidyasagar, K. (1999). *Inorg. Chem.* **38**, 1394–1400.
Basso, R., Lucchetti, G., Zefiro, L. & Palenzona, A. (1996). *Eur. J. Mineral.* **8**, 487–492.
Bayliss, P. & Nowacki, W. (1972). *Z. Kristallogr.* **135**, 308–315.
Becke, A. D. & Edgecombe, K. E. (1990). *J. Chem. Phys.* **92**, 5397–5403.
Bickmore, B. R., Wander, M. F. C., Edwards, J., Maurer, J., Shepherd, K., Meyer, E., Johansen, W. J., Frank, R. A., Andros, C. & Davis, M. (2013). *Am. Mineral*, **98**, 340–349.
Brese, N. E. & O'Keeffe, M. (1991). *Acta Cryst.* B**47**, 192–197.
Brown, I. D. (1978). *Chem. Soc. Rev.* **7**, 359–378.
Brown, I. D. (2002). *The Chemical Bond in Inorganic Chemistry: The Bond Valence Model*, p. 278. Oxford University Press.
Brown, I. D. (2006). *Acta Cryst.* B**62**, 692–694.
Brown, I. D. (2009). *Chem. Rev.* **109**, 6858–6919.
Brown, I. D. (2011). *J. Phys. Chem. A*, **115**, 12638–12645.
Brown, I. D. (2013*a*). *Struct. Bond.* doi: 10.1007/430_2012_83.
Brown, I. D. (2013*b*). *Am. Mineral.* **98**, 1093–1094.
Brown, I. D. & Altermatt, D. (1985). *Acta Cryst.* B**41**, 244–247.
Brown, I. D. & Wu, K. K. (1976). *Acta Cryst.* B**32**, 1957–1959.
Burns, P. C., Clark, C. M. & Gault, R. A. (2000). *Can. Mineral.* **38**, 809–816.
Cachau-Herreillat, D., Norbert, A., Maurin, M. & Philippot, E. (1981). *J. Solid State Chem.* **37**, 352–361.
Castro, A., Enjalbert, R., Lloyd, D., Rasines, I. & Galy, J. (1990). *J. Solid State Chem.* **85**, 100–107.
Champarnaud-Mesjard, J., Frit, B., Chagraoui, A. & Tairi, A. (1996). *J. Solid State Chem.* **127**, 248–255.
Christy, A. G., Grew, E. S., Mayo, S. C., Yates, M. G. & Belakovskiy, D. I. (1998). *Mineral. Mag.* **62**, 77–92.
Cooper, M. A. & Hawthorne, F. C. (1996). *Can. Mineral.* **34**, 821–826.
Daniel, F., Moret, J., Maurin, M. & Philippot, E. (1981). *Acta Cryst.* B**37**, 1278–1281.
Daniel, F., Moret, J., Maurin, M. & Philippot, E. (1982). *Acta Cryst.* B**38**, 703–706.
Dytyatev, O. & Dolgikh, V. (1999). *Mater. Res. Bull.* **34**, 733–740.
Elerman, Y. (1993). *Doga. Turk. J. Phys*, **17**, 465–473.
Feger, C. R., Schimek, G. L. & Kolis, J. W. (1999). *J. Solid State Chem.* **143**, 246–253.
Gillespie, R. J. & Nyholm, R. S. (1957). *Q. Rev. Chem. Soc.* **11**, 339.
Goldschmidt, V. M. (1926). *Geochemische Verteilungsgesetze der Elemente*. VII. Die Gesetze der Kristallchemie. *Skr. Norske Vidensk.-Akad. i Oslo*, **2**, 1–117.
Grzechnik, A. & Friese, K. (2010). *J. Phys. Condens. Matter*, **22**, 095402.
Guesdon, A. & Raveau, B. (2000). *Chem. Mater.* **12**, 2239–2243.
Harvey, M. A., Baggio, S. & Baggio, R. (2006). *Acta Cryst.* B**62**, 1038–1042.
Hottentot, D. & Loopstra, B. O. (1983). *Acta Cryst.* C**39**, 320–322.
Hyde, B. G. & Andersson, S. (1989). *Inorganic Crystal Structures*, 430 pp. New York: John Wiley and Sons.
Johansson, G. B. (1978). *Acta Cryst.* B**34**, 2830–2832.
Kampf, A. R., Mills, S. J., Housley, R. M., Marty, J. & Thorne, B. (2010). *Am. Mineral*, **95**, 1569–1573.
Krämer, V. & Brandt, G. (1985). *Acta Cryst.* C**41**, 1152–1154.
Krämer, V. & Brandt, G. (1986). *Acta Cryst.* C**42**, 917–918.
Krivovichev, S. V. & Brown, I. D. (2001). *Z. Kristallogr.* **216**, 245–247.
Lalik, E. (2005). *J. Appl. Cryst.* **38**, 152–157.
Lindqvist, O. (1968). *Acta Chem. Scand.* **22**, 977–982.
Lindqvist, O. (1972). *Acta Chem. Scand.* **26**, 1423–1430.
Loopstra, B. O. & Goubitz, K. (1986). *Acta Cryst.* C**42**, 520–523.
Lundegaard, L. F., Makovicky, E., Boffa-Ballaran, T. & Balić-Žunić, T. (2005). *Phys. Chem. Miner.* **32**, 578–584.
Lundegaard, L. F., Miletich, R., Balić-Žunić, T. & Makovicky, E. (2003). *Phys. Chem. Miner.* **30**, 463–468.
Makovicky, E. & Balić-Žunić, T. (1998). *Acta Cryst.* B**54**, 766–773.
Meunier, G., Frit, B. & Galy, J. (1976). *Acta Cryst.* B**32**, 175–180.
Miletich, R. (1993). *Miner. Petrol*, **48**, 129–145.
Miletich, R. & Pertlik, F. (1998). *J. Alloys Compd.* **268**, 107–111.
Mills, S. J. & Christy, A. G. (2013). *Acta Cryst.* B**69**, 145–149.
Mills, S. J., Christy, A. G., Chen, E. C.-C. & Raudsepp, M. (2009). *Z. Kristallogr.* **224**, 423–431.
Mills, S. J., Hatert, F., Nickel, E. H. & Ferraris, G. (2009). *Eur. J. Mineral.* **21**, 1073–1080.
Mills, S. J., Kampf, A. R., Raudsepp, M. & Christy, A. G. (2009). *Mineral. Mag.* **73**, 837–845.
Mills, S. J., Kartashov, P. M., Kampf, A. R. & Raudsepp, M. (2010). *Eur. J. Mineral.* **22**, 613–621.
Mills, S. J. & Nestola, F. (2012). *Mineral. Mag.* **76**, 975–985.
Olsen, L. A., Balić-Zunić, T. & Makovicky, E. (2008). *Inorg. Chem.* **47**, 6756–6762.
Olsen, L. A., Friese, K., Makovicky, E., Balić-Žunić, T., Morgenroth, W. & Grzechnik, A. (2011). *Phys. Chem. Miner.* **38**, 1–10.
Perez, G., Lasserre, F., Moret, J. & Maurin, M. (1976). *J. Solid State Chem.* **17**, 143–149.
Pertlik, F. (1972). *Tschermaks Mineral. Petrogr. Mitt.* **18**, 39–55.
Philippot, E., Astier, R., Loeksmanto, W., Maurin, M. & Moret, J. (1978). *Rev. Chim. Miner.* **15**, 283–291.
Platte, C. & Trömel, M. (1981). *Acta Cryst.* B**37**, 1276–1278.
Raulot, J., Baldinozzi, G., Seshadri, R. & Cortona, P. (2002). *Solid State Sci.* **4**, 467–474.
Robinson, K., Gibbs, G. V. & Ribbe, P. H. (1970). *Science*, **172**, 567–570.
Seshadri, R. (2001). *Proc. Indian Acad. Sci. Chem. Sci.* **113**, 487–496.
Sidgwick, N. V. & Powell, H. M. (1940). *Proc. R. Soc. London*, **176**, 153–180.
Topa, D., Makovicky, E., Balić-Žunić, T. & Paar, W. H. (2003). *Can. Mineral.* **41**, 1155–1166.
Urusov, V. S. (2003). *Z. Kristallogr.* **218**, 709–719.
Urusov, V. S. (2006). *Dokl. Phys. Chem.* **408**, 137–141.
Zachara, J. (2007). *Inorg. Chem.* **46**, 9760–9767.
Zachariasen, W. H. (1949). *Acta Cryst.* **2**, 291–296.